Hindawi Publishing Corporation
Journal of Nanomaterials
Volume 2014, Article ID 690514, 6 pages
http://dx.doi.org/10.1155/2014/690514

Research Article

Synthesis and Catalytic Performance of Graphene Modified CuO-ZnO-Al_2O_3 for CO_2 Hydrogenation to Methanol

Zheng-juan Liu,[1,2] Xing-jiang Tang,[1] Shan Xu,[1] and Xiao-lai Wang[1]

[1] *State Key Laboratory for Oxo Synthesis and Selective Oxidation, Lanzhou Institute of Chemical Physics, Chinese Academy of Sciences, Lanzhou 730000, China*
[2] *University of Chinese Academy of Sciences, Beijing 100049, China*

Correspondence should be addressed to Shan Xu; xushan@licp.cas.cn

Received 3 July 2014; Accepted 25 July 2014; Published 24 August 2014

Academic Editor: Tifeng Jiao

CuO-ZnO-Al_2O_3 and graphene nanosheet (GNS) were synthesized by coprecipitation route and reduction of exfoliated graphite oxides method, respectively. GNS modified CuO-ZnO-Al_2O_3 nanocomposites were synthesized by high energy ball milling method. The structure, morphology, and character of the synthesized materials were studied by BET, XRD, TEM, and H_2-TPR. It was found that by high energy ball milling method the CuO-ZnO-Al_2O_3 nanoparticles were uniformly dispersed on GNS surfaces. The catalytic performance for the methanol synthesis from CO_2 hydrogenation was also tested. It was shown experimentally that appropriate incorporation of GNS into the CuO-ZnO-Al_2O_3 could significantly increase the catalyst activity for methanol synthesis. The 10 wt.% GNS modified CuO-ZnO-Al_2O_3 catalyst gave a methanol space time yield (STY) of 92.5% higher than that on the CuO-ZnO-Al_2O_3 catalyst without GNS. The improved catalytic performance was attributed to the excellent promotion of GNS to dispersion of CuO and ZnO particles.

1. Introduction

The concentration of atmospheric CO_2 had risen from ~280 ppm before 1860 to ~390 ppm in 2010, which is further predicted to be ~570 ppm by the end of the century [1]. The increase in CO_2 emissions arguably causes to the increase in global temperatures and climate changes, which is called the "greenhouse effect." Hence, the comprehensive utilization of CO_2 has drawn more and more attention from the entire world. Because converting CO_2 to methanol not only could promote the efficient utilization of CO_2 but also has found a new way of methanol production, CO_2 hydrogenation to methanol has become a hot topic of academic research [2]. But due to the fact that CO_2 is inert molecule and very difficult to be activated, so making an appropriate catalyst that could bring the enhancement of CO_2 conversion and methanol yield will be the key topic of this research.

A conventional CuO-ZnO-Al_2O_3 catalyst for methanol production from synthesis gas (mixture of CO, CO_2, and H_2) is now accepted [3–5]. But it is not adequate for methanol synthesis from a H_2/CO_2 mixture at temperatures below 250°C [6–8]. Hence, several modifications have been used to improve conventional CuO-ZnO-Al_2O_3 methanol synthesis catalysts. The key is to keep a high dispersion of the Cu/Zn crystallites where the active sites are as stated in [9, 10]. A lot of works have been done by doping other metal elements in CuO-ZnO-based catalyst for investigation, for example, Cr, Zr, V, Ce, Ti, Ga, and Pd [11–13]. In addition, some works tried to find the suitable method to synthsis CuO-ZnO-Al_2O_3 catalyst, such as sol-gel, hydrothermal, reverse microemulsion, and organic chelating agent to the common coprecipitation method [14, 15].

In comparison to the other preparation techniques, high energy ball milling has been used as an effective and easy method for preparation of high dispersed and refining grains including nanocrystalline as well as amorphous materials [16]. High energy ball milling process can change not only the size but also the structure of the material, so that makes

the active species in the secondary distribution of the sample surface [17, 18]; moreover, the particles undergo heavy pressure and mechanical deformation forming high-density fault structure and high concentration of lattice defects [19]. As a result, it makes the catalytic activity significantly improves due to the dynamic performance of the catalyst increasing.

Graphene nanosheet (GNS) is considered an excellent catalytic carrier and additives owing to its unique physical chemical properties [20], such as, special electronic transmission characteristics, huge specific surface area, and excellent electrical and thermal conductivity. So far, the research of graphene in catalyst fields primarily appears to be on photoelectric catalysis, fuel cell, lithium ion battery, and so on.

In this paper, we doped GNS with CuO-ZnO-Al_2O_3 composite oxides by high energy ball milling method. The prepared catalysts exhibit high dispersion of nanocomposite particles and high activity for CO_2 hydrogenation to methanol.

2. Experimental

2.1. Material Synthesis. Graphene nanosheet (GNS) was synthesized by reduction of graphite oxides. Firstly, we prepare graphite oxide by a modified Hummers method [21]. Then, the prepared graphite oxide was dispersed in deionized water, followed by ultrasonic as graphene suspension and the hydrazine hydrate was added as the reducing agent. After that the mixture was refluxed at 100°C. In the end, GNS was obtained after filtering, washing, and drying the resulting mixture.

The mixed aqueous solution of $Cu(NO_3)_2$, $Zn(NO_3)_2$, and $Al(NO_3)_3$ (the mole ratio is 6 : 3 : 1) with a total concentration of 1 mol/L and the aqueous solution of 1 mol/L Na_2CO_3 were prepared. The CuO-ZnO-Al_2O_3 catalysts were prepared by concurrently dropping Na_2CO_3 solution and mixed nitrates solution into an around-bottomed flask at 70°C under the water bath with vigorous stirring. The mixed nitrates solution was dropped at a rate of 5 mL/min and the pH was kept constant at 7-8. Then, the precursor was filtered and washed followed by dried overnight at 80°C. Finally the precursor was calcined at 350°C for 6 h to produce the CuO-ZnO-Al_2O_3 catalysts.

In our experiment Fritsch 7 Pulverisette planetary ball mill was applied. The anhydrous ethanol was used as ball mill solvent and WC balls (Φ = 10 mm) were used as grinding balls. The milling rotational speed was 500 r/min. And ball mill could stop running for 15 min after working for 30 min. The cumulative milling time is 6 h. The mixture was dried at 60°C for 24 h after ball milling. The catalysts are denoted as CZA (without GNS), 5G-CZA (5 wt.% GNS), 10G-CZA (10 wt.% GNS), and 15G-CZA (15 wt.% GNS), respectively, in terms of graphene contents variations.

2.2. Material Characterization. Panalytical X'Pert Pro polycrystal X-ray diffraction (XRD) was performed with Cu-Kα radiation, λ = 0.15406 nm, tube voltage being 40 kV, and tube current being 40 mA in crystal structure of material characterization. The grain size of material is calculated by the Scherrer formula based on the strongest half peak width of the diffraction peak. The Brunauer-Emmett-Teller (BET) surface area of the catalyst was measured with an ASAP-2010 surface analyzer. The samples were degassed at approximately 200°C for 4 h before analysis. Hydrogen temperature-programmed reduction (H_2-TPR) was conducted with a GC-7890II Gas chromatograph equipped with a thermal conductive detector (TCD) made from Shanghai Tianmei Company. The quality of the catalyst tested was 10 mg with the 5% H_2-N_2 mixture gas as the reducing gas at a flow rate of 50 mL/min and heating rate of 10°C/min. Tecnai G2-F30 transmission electron microscopy (TEM) was used to test the morphology of catalyst with 300 kV accelerating voltage.

2.3. Catalytic Tests. The activity tests were carried out in a stainless steel fixed bed microreactor. The catalyst (20–40 mesh size, 0.5 g) was packed into a stainless steel fixed bed microreactor (15 mm Φ) and reduced in a mixed ($V(H_2)/V(N_2)$ = 5/95) flow at 280°C for 6 h. After the reduction, the gas feed was switched to the reactant gas ($V(H_2)/V(CO_2)/V(N_2)$ = 69/23/8). The reaction was tested at a pressure of 3.0 MPa and temperature of 250°C with a space velocity of 12000 mL/h·$g_{catal.}$. The CO_2 and CO were separated and regulated by carbon packed molecular sieve column and thermal conductivity detector (TCD). Methanol and other organic matters were separated and regulated by PoraPak Q column and hydrogen flame ionization detector (FID).

3. Results and Discussion

3.1. Structure Properties of Catalysts. The XRD patterns of the pure CuO-ZnO-Al_2O_3 samples and the CuO-ZnO-Al_2O_3 doped by varying contents of GNS samples are compared in Figure 1. No matter how much is the amount of GNS added in the samples, the characteristic diffraction peaks of CuO appeared at 2θ = 35.6°, 38.8°, and 48.9° and the ZnO special diffraction peaks appeared at 2θ = 31.8°, 34.5°, and 36.3° in all the samples. The peak at 2θ = 26° is the typical diffraction peak (002) of graphite material. With the added GNS increasing, the typical diffraction peak (002) intensity weakened a lot compared with the natural graphite. As part of the crystal structure of the incomplete oxidation of flake graphite damaged to some extent, so that its peak intensity is greatly decreased.

The physicochemical properties of CuO-ZnO-Al_2O_3 doped with different amounts of GNS are summarized in Table 1. For comparison, the physicochemical properties of pure CuO-ZnO/Al_2O_3 are also included. The surface areas of CZA, 5G-CZA, 10G-CZA, and 15G-CZA are 40.9, 113.3, 147.8, and 186.3 m^2/g, respectively. The surface areas of the samples increase with the increase of GNS doping amount and it proves that specific surface area of sample is proportional to the GNS addition. From Table 1, we could get the crystallite size data of CuO and ZnO calculated from their corresponding diffraction peak by Scherrer equation. And

Table 1: Physicochemical properties of CuO-ZnO-Al_2O_3 doped with different amounts of GNS.

Catalysts	Surface area (m^2/g)	CuO crystallite size (nm)	ZnO crystallite size (nm)
CZA	40.9	13.6	17.3
5G-CZA	113.3	12.6	16.4
10G-CZA	147.8	12.4	14.0
15G-CZA	186.3	14.5	20.6

CuO and ZnO crystallite sizes were calculated from XRD data using Scherrer equation.

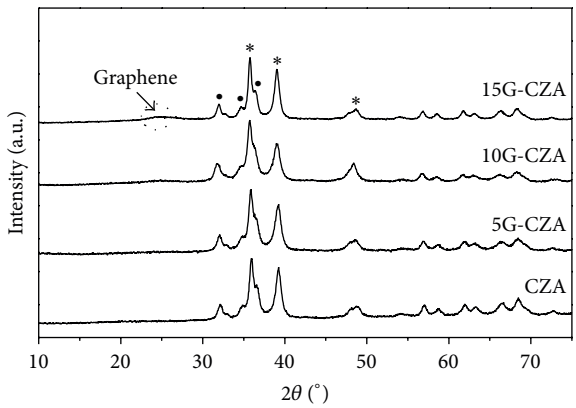

Figure 1: XRD patterns of CuO-ZnO-Al_2O_3doped with different amounts of GNS [∗] CuO; [•] ZnO.

the crystallite size of CuO particles decreased from 13.6 nm of CZA to 12.4 nm of 10G-CZA and the size of ZnO particles decreased from 18.3 nm to 14.0 nm. When milling time was constant, the minimum crystallite size of the samples is the sample powder with 10 wt.% GNS doped. For this result, there might be two reasons: (1) the CuO-ZnO/Al_2O_3 particles adsorb on the surface of GNS, which reduce the surface energy of the particles and prevent the recombination between breaking chemical bonds, leading to the decrease of mechanical strength of the particles and the external force for dislocation extension and finally resulting in reinforcement of the crushing effect. (2) The compatibility of the powder with ethanol increases by the addition of GNS, which improves the rheological properties of the slurry. As a result, the slurry viscosity is decreased and the fluidity and dispersal ability of particles are promoted making the collision frequency between the ball mill and powder particle higher. However, for the sample with 15 wt.% GNS doped the crystallite size of CuO increased to 14.5 nm and the size of ZnO increased to 20.6 nm. This result illustrates the excessive addition of graphene reduced the collision frequency between the ball mill and particles, so that the particles were bigger for aggregating. Such a conclusion suggests that crystallite size is the smallest when GNS doped in the composite is 10 wt.% and the crushing grain effect is weakened over this doped amount.

3.2. TEM. The morphology of CuO-ZnO/Al_2O_3 doped with different amounts of GNS is shown in the TEM images in Figure 2. In Figure 2(a), the particle sizes are larger with obvious agglomeration of the pure CuO-ZnO-Al_2O_3 catalysts which could be seen after ball milling. In Figures 2(b), 2(c), and 2(e), the transparent cicada's wing shape of nanographene sheets characteristic could be seen and the composite metal oxides particles are evenly distributed on the GNS. The stacks of graphene layers are clearly observed in the high-resolution image of Figure 2(d). Due to the fact that the GNS has a large specific surface area and the big π electron delocalization system, it is beneficial to the anchoring of the metal oxide nanoparticles and increases the electrostatic repulsion between the particles. GNS made by chemical reduction method has a certain amount of lattice defects and some residual oxygen functional groups making the distribution of the catalyst nanoparticles more uniform. The ball mill method made the metal oxide particles distributed evenly on GNS with the shape more regular and the size smaller. Figure 2(c) shows the CuO-ZnO-Al_2O_3 catalysts doped with 10 wt.% GNS with the smallest size distributed on the GNS sheets most uniformly which is consistent with the change of the grain size of CuO and ZnO.

3.3. Reduction Properties of the Catalysts. The H_2-TPR patterns of CuO-ZnO/Al_2O_3 doped with different amounts of GNS are given in Figure 3 and the four samples are all reduced in the temperature range of 150–290°C. For the pure CuO-ZnO/Al_2O_3 catalyst, there is a big side-by-side peak which can be decomposed into two peaks noted as β and γ, respectively. Because ZnO and Al_2O_3 are not reduced under the experimental conditions described here [22], so the two peaks appeared in the TPR profile stand for CuO existing in two different ways. The low temperature reduction peak (β peak) is assigned to reduction of CuO highly dispersed on the surface of catalysts and the high temperature reduction peak (γ peak) is assigned to reduction of CuO in bulk phase. It is noticeable that there is a new small peak appearing at lower temperature in the H_2-TPR patterns of other three samples doped with GNS. We name the lower temperature peak as α peak and assume that it is the contribution of GNS. GNS makes the shifts of reduction peak of the highly dispersed CuO toward lower temperature; that is, it makes part of CuO being more easily reduced by H_2. This is because GNS has high adsorption and activation ability for hydrogen species [23] and implies that in the reaction GNS is not only a carrier but also a good promoter. In order to prove that the appearance of α peak has nothing to do with the reduction of GNS, we run a H_2-TPR test in the same steps as before to pure GNS, getting a curve which is almost a straight line parallel to the baseline without any peaks. The areas of reduction peaks and their contributions to the TPR pattern over catalysts are given in Table 2. We can see that the proportion of areas of α and β peaks together is as high as 69.1% when the amounts of GNS doped is 10 wt.% indicating a higher content of highly dispersed CuO. The result is in accordance with the conclusion of aforementioned XRD, TEM characterization.

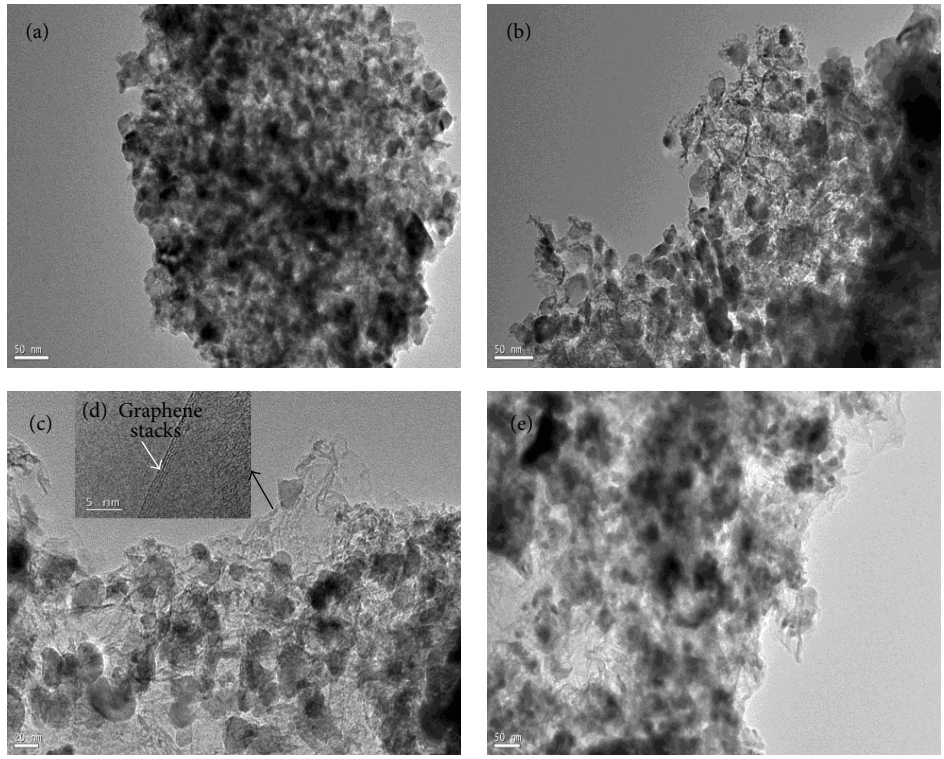

Figure 2: TEM photos of CuO-ZnO/ Al_2O_3 doped with different amounts of GNS: (a) CZA, (b) 5G-CZA, (c) 10G-CZA, (d) the HRTEM photos of 10G-CZA, and (e) 15G-CZA.

Table 2: Temperatures of reduction peaks and their contributions to the TPR pattern over catalysts.

Catalysts	T_α (°C)	T_β (°C)	T_γ (°C)	$(A_\alpha + A_\beta)/(A_\alpha + A_\beta + A_\gamma)$ (%)
CZA	—	215	240	43.8
5G-CZA	197	224	245	58.7
10G-CZA	204	227	246	69.1
15G-CZA	215	230	249	56.0

A_α, A_β, and A_γ represent the areas of α, β, and γ peaks, respectively.

3.4. The Performance and Stability of the Catalysts. The activity evaluation of CO_2 hydrogenation to methanol is carried out in the fixed bed microreactor and methanol and CO are the main carbonaceous products with a small amount of CH_4. In Table 3, the copper dispersion (D_{Cu}) and active surface area (MSA) of the catalysts are showed by calculation from N_2O chemisorption data. We could find that D_{Cu} and MSA values are increased with the amount of the GNS increased till 10 wt.%, and then those are reduced when the GNS amount is up to 15 wt.%. As shown in Table 3, the CO_2 conversion and methanol space time yield (STY) are in accordance with D_{Cu} and MSA. The 10G-CZA has the highest CO_2 conversion and STY of 14.6% and 360 mg/g·h, which are 71.8% and 92.5% higher than that on the CZA catalyst, respectively. These results suggest that the dispersion and particle size of active components of CuO and ZnO have a significant influence on the catalytic activity. The 10G-CZA catalyst, which has the most highly dispersion and the smallest particle size, is most conducive to the improvement of the catalytic performance. The result is in agreement with the XRD, TEM, and H_2-TPR and other analysis conclusions.

Figure 4 shows the assay results of conversion and methanol selectivity at 230–280°C over the catalysts of CZA and 10G-CZA. The CO_2 conversion of the both catalysts went up as the temperature increased because appropriately raising the reaction temperature could promote the CO_2 reaction. On the other hand, both the methanol selectivity decreased with the temperature increased because the methanol formation from the hydrogenation of CO_2 is thermodynamically restricted within low conversion under the operating conditions [24]. It can be showed that the CO_2 conversion and the methanol selectivity of 10G-CZA catalyst were always higher than that of the CZA catalyst, confirming that graphene is an excellent promoter for CuO-ZnO-Al_2O_3 catalysts on CO_2 hydrogenation to methanol.

The 10G-CZA as the best catalyst performance was selected for the stability test, and the results are shown in Figure 5. The CO_2 conversion and methanol selectivity

Table 3: Catalytic properties and N_2O chemisorption data of CuO-ZnO-Al_2O_3 doped with different amounts of GNS.

Catalysts	D_{Cu} (%)	MSA (m^2/g_{Cu})	Conversion of CO_2 (%)	Selectivity of CH_3OH (%)	STY of CH_3OH (mg/g·h)
CZA	7.2	10.8	8.5	55.7	187
5G-CZA	8.2	11.7	12.1	59.9	287
10G-CZA	9.4	12.6	14.6	62.3	360
15G-CZA	7.7	11.3	12.3	57.7	281

Reaction conditions: temperature = 250°C; pressure = 3.0 MPa; SV = 12000 ml/h·g_{catal}.

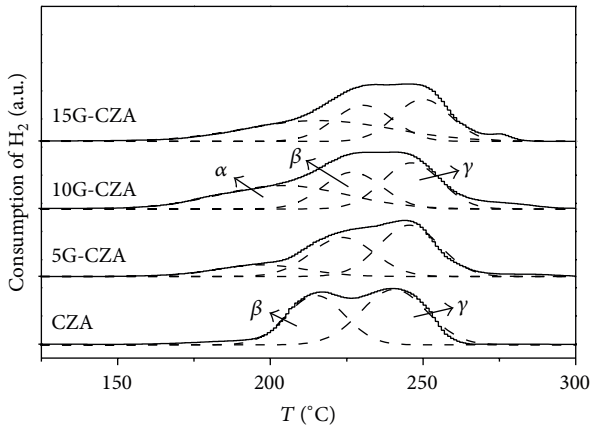

Figure 3: H_2-TPR patterns of CuO-ZnO-Al_2O_3 doped with different amounts of GNS.

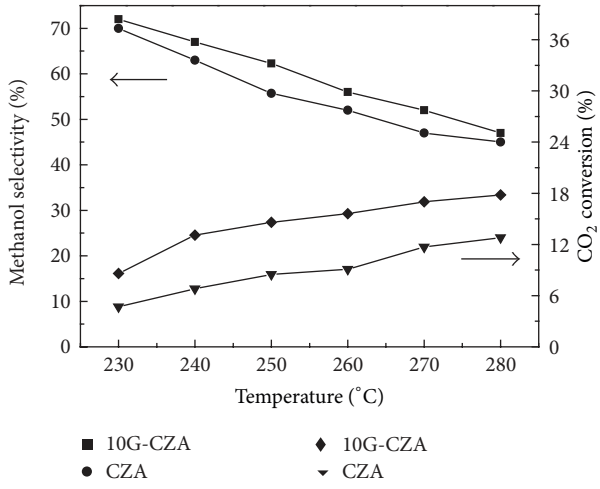

Figure 4: Variation of CO_2 conversion and methanol selectivity with reaction temperature over CZA and 10G-CZA catalyst (P = 3.0 MPa, SV = 12000 mL/h·$g_{catal.}$).

of 10G-CZA catalyst remain unchanged after continuous operation for 30 h in the fixed bed microreactor under T = 250°C, P = 3.0 MPa, and SV = 12000 mL/h·$g_{catal.}$. The results show that the catalyst prepared by ball milling method has very good stability.

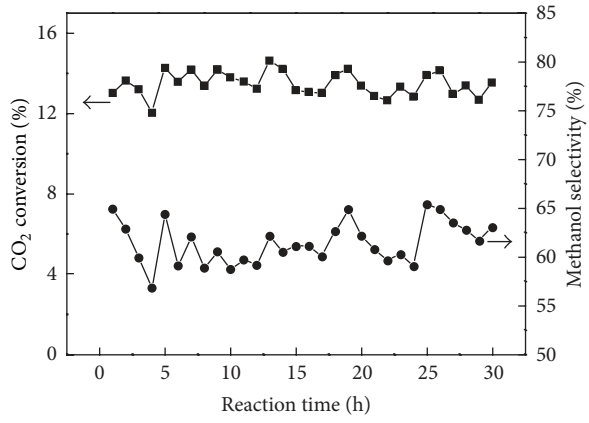

Figure 5: Variation of CO_2 conversion and methanol selectivity with reaction time over 10G-CZA catalyst (T = 250°C, P = 3.0 MPa, SV = 12000 mL/h·$g_{catal.}$).

4. Conclusions

The high energy ball milling method has been used to prepare GNS modified CuO-ZnO-Al_2O_3 nanocomposites catalysts for methanol synthesis from CO_2 hydrogenation. GNS/CuO-ZnO-Al_2O_3 nanocomposites catalyst with 10 wt.% GNS showed the best catalytic activity with CO_2 conversion and methanol space time yield is 71.8% and 92.5% higher separately than the catalyst without GNS addition. The GNS modified CuO-ZnO-Al_2O_3 nanocomposites catalysts prepared by high energy ball milling method make the dispersion of active components of CuO and ZnO higher and smaller particle size and exhibit a much enhancement in catalytic performance. The ball mill operation is simple with low energy consumption, environmentally friendly, and suitable for large-scale preparation of industrialization.

Conflict of Interests

The authors declared that they have no conflict of interests regarding this paper.

Acknowledgments

This work was financially supported by the National Natural Science Foundation of China (no. 21103205) and the "Western Light" Project (2013) of Chinese Academy of Sciences.

References

[1] X. Xiaoding and J. A. Moulijn, "Mitigation of CO_2 by chemical conversion: plausible chemical reactions and promising products," *Energy and Fuels*, vol. 10, no. 2, pp. 305–325, 1996.

[2] G. A. Olah, A. Goeppert, and G. K. S. Prakash, "Chemical recycling of carbon dioxide to methanol and dimethyl ether: from greenhouse gas to renewable, environmentally carbon neutral fuels and synthetic hydrocarbons," *Journal of Organic Chemistry*, vol. 74, no. 2, pp. 487–498, 2009.

[3] F. Pontzen, W. Liebner, V. Gronemann, M. Rothaemel, and B. Ahlers, "CO_2-based methanol and DME—efficient technologies for industrial scale production," *Catalysis Today*, vol. 171, no. 1, pp. 242–250, 2011.

[4] Z. Hong, Y. Cao, J. Deng, and K. Fan, "CO_2 hydrogenation to methanol over $Cu/ZnO/Al_2O_3$ catalysts prepared by a novel gel-network-coprecipitation method," *Catalysis Letters*, vol. 82, no. 1-2, pp. 37–44, 2002.

[5] K. Jun, W. Shen, K. S. Rama Rao, and K. Lee, "Residual sodium effect on the catalytic activity of $Cu/ZnO/Al_2O_3$ in methanol synthesis from CO_2 hydrogenation," *Applied Catalysis A: General*, vol. 174, no. 1-2, pp. 231–238, 1998.

[6] X. Liu, G. Q. Lu, Z. Yan, and J. Beltramini, "Recent Advances in Catalysts for Methanol Synthesis via Hydrogenation of CO and CO_2," *Industrial and Engineering Chemistry Research*, vol. 42, no. 25, pp. 6518–6530, 2003.

[7] J. L. G. Fierro, I. Melián-Cabrera, and M. López Granados, "Reverse topotactic transformation of a Cu-Zn-Al catalyst during wet Pd impregnation: Relevance for the performance in methanol synthesis from CO_2/H_2 mixtures," *Journal of Catalysis*, vol. 210, no. 2, pp. 273–284, 2002.

[8] J. L. G. Fierro, I. Melián-Cabrera, and M. López Granados, "Pd-modified Cu-Zn catalysts for methanol synthesis from CO_2/H_2 mixtures: catalytic structures and performance," *Journal of Catalysis*, vol. 210, no. 2, pp. 285–294, 2002.

[9] J. Wang, S. Funk, and U. Burghaus, "Indications for metal-support interactions: the case of CO_2 adsorption on Cu/ZnO(0001)," *Catalysis Letters*, vol. 103, no. 3-4, pp. 219–223, 2005.

[10] V. E. Ostrovskii, "Mechanisms of methanol synthesis from hydrogen and carbon oxides at Cu-Zn-containing catalysts in the context of some fundamental problems of heterogeneous catalysis," *Catalysis Today*, vol. 77, no. 3, pp. 141–160, 2002.

[11] I. Melián-Cabrera, M. L. Granados, and J. L. G. Fierro, "Effect of Pd on Cu-Zn catalysts for the hydrogenation of CO_2 to methanol: Stabilization of Cu metal against CO_2 oxidation," *Catalysis Letters*, vol. 79, no. 1–4, pp. 165–170, 2002.

[12] S. Schuyten and E. E. Wolf, "Selective combinatorial studies on Ce and Zr promoted Cu/Zn/Pd catalysts for hydrogen productio via methanol oxidative reforming," *Catalysis Letters*, vol. 106, no. 1-2, pp. 7–14, 2006.

[13] I. Melián-Cabrera, M. López Granados, and J. L. G. Fierro, "Structural reversibility of a ternary $CuO\text{-}ZnO\text{-}Al_2O_3$ ex hydrotalcite-containing material during wet Pd impregnation," *Catalysis Letters*, vol. 84, no. 3-4, pp. 153–162, 2002.

[14] G. Busca, U. Costantino, F. Marmottini et al., "Methanol steam reforming over ex-hydrotalcite Cu-Zn-Al catalysts," *Applied Catalysis A: General*, vol. 310, no. 1-2, pp. 70–78, 2006.

[15] X. Zhang, L. Wang, C. Yao et al., "A highly efficient $Cu/ZnO/Al_2O_3$ catalyst via gel-coprecipitation of oxalate precursors for low-temperature steam reforming of methanol," *Catalysis Letters*, vol. 102, no. 3-4, pp. 183–190, 2005.

[16] M. Varga, Á. Molnár, G. Mulas, M. Mohai, I. Bertóti, and G. Cocco, "Cu-MgO samples prepared by mechanochemistry for catalytic application," *Journal of Catalysis*, vol. 206, no. 1, pp. 71–81, 2002.

[17] V. A. Zazhigalov, J. Haber, J. Stoch, L. V. Bogutskaya, and I. V. Bacherikova, "Mechanochemistry as activation method of the V-P-O catalysts for n-butane partial oxidation," *Applied Catalysis A: General*, vol. 135, no. 1, pp. 155–161, 1996.

[18] S. Mori, W.-C. Xu, T. Ishidzuki, N. Ogasawara, J. Imai, and K. Kobayashi, "Mechanochemical activation of catalysts for CO_2 methanation," *Applied Catalysis A: General*, vol. 137, no. 2, pp. 255–268, 1996.

[19] C. Feng, G. Fan, and Y. Wang, "Progress in synthesis methods of ceria-based oxygen storage materials for automotive catalysts," *Modern Chemical Industry*, vol. 24, no. 11, pp. 10–14, 2004.

[20] Y. Lu, M. Zhou, C. Zhang, and Y. Feng, "Metal-embedded graphene: a possible catalyst with high activity," *Journal of Physical Chemistry C*, vol. 113, no. 47, pp. 20156–20160, 2009.

[21] W. S. Hummers Jr. and R. E. Offeman, "Preparation of graphitic oxide," *Journal of the American Chemical Society*, vol. 80, no. 6, p. 1339, 1958.

[22] E. Samei, M. Taghizadeh, and M. Bahmani, "Enhancement of stability and activity of $Cu/ZnO/Al_2O_3$ catalysts by colloidal silica and metal oxides additives for methanol synthesis from a CO_2-rich feed," *Fuel Processing Technology*, vol. 96, pp. 128–133, 2012.

[23] A. Ghosh, K. S. Subrahmanyam, K. S. Krishna et al., "Uptake of H_2 and CO_2 by graphene," *The Journal of Physical Chemistry C*, vol. 112, no. 40, pp. 15704–15707, 2008.

[24] W. Shen, K. Jun, H. Choi, and K. Lee, "Thermodynamic Investigation of Methanol and Dimethyl Ether Synthesis from CO_2 Hydrogenation," *Korean Journal of Chemical Engineering*, vol. 17, no. 2, pp. 210–216, 2000.